The Journal of Neuroscience, February 1993, 13(2): 660–673

# Modal Gating of $Na^+$ Channels as a Mechanism of Persistent $Na^+$ Current in Pyramidal Neurons from Rat and Cat Sensorimotor Cortex

**Christian Alzheimer, Peter C. Schwindt, and Wayne E. Crill**

Department of Physiology and Biophysics, School of Medicine, University of Washington, Seattle, Washington 98195

**The kinetic behavior of brain $Na^+$ channels was studied in pyramidal cells from rat and cat sensorimotor cortex using either the thin slice preparation or acutely isolated neurons. Single-channel recordings were obtained in the cell-attached and inside-out configuration of the patch-clamp technique. $Na^+$ channels had a conductance of about 16 pS. Patches always contained several $Na^+$ channels, usually 4–12. In both preparations, long depolarizing pulses revealed two distinct patterns of late $Na^+$ channel activity following transient openings. (1) $Na^+$ channels displayed sporadic brief late openings sometimes clustered to "minibursts" of 10–40 msec. These events occurred at a low frequency, yielding open probability ($NP_o$) values below 0.01 (mean = 0.0034). (2) In the second gating mode, an individual $Na^+$ channel in the patch failed to inactivate and produced a burst of openings often lasting to the end of the pulse. This behavior was observed in about 1% of depolarizations. Shifts to the bursting mode were usually confined to a single 400 msec pulse, but rarely occurred during two or more consecutive pulses applied at 2 sec intervals. Sustained bursts did not require preceding transient openings to occur since they were also observed during slow depolarizing voltage ramps. The similar incidence of inactivation failures in cell-attached versus inside-out recordings suggests that the bursting mode is a property of the channel and/or adjacent membrane-bound structures. Calculations indicate that brief late openings and rare sustained bursts suffice to generate a small but significant whole-cell current. Since the $Na^+$ channels mediating early, brief late, and sustained openings were identical in terms of their elementary electrical properties, we propose that the fast and the persistent $Na^+$ currents of cortical pyramidal cells are generated by an electrophysiologically uniform population of $Na^+$ channels that can individually switch between different gating modes.**

***[Key words: $Na^+$ channels, modal gating, persistent $Na^+$ current, single-channel recordings, rat and cat sensorimotor cortex, thin slice, acutely isolated neurons]***

The basic function of voltage-dependent $Na^+$ currents is the generation and propagation of action potentials (Hille, 1992), but recordings from muscular, cardiac, and neuronal tissues have shown that, in addition to the fast, rapidly inactivating $Na^+$ current, several excitable cells are also endowed with a noninactivating, TTX-sensitive $Na^+$ conductance (e.g., Attwell et al., 1979; Llinás and Sugimori, 1980; Stafstrom et al., 1982, 1985; Patlak and Ortiz, 1985, 1986; McCormick and Prince, 1987; Alonso and Llinás, 1989; Gage et al., 1989; French et al., 1990). Within the mammalian CNS, a slowly or noninactivating (persistent) $Na^+$ current ($I_{NaP}$) has been found in neurons from several brain regions including neocortex, entorhinal cortex, hippocampus, thalamus, and cerebellum (for review, see Llinás, 1988). A prominent $I_{NaP}$ has been observed in layer V neurons from cat sensorimotor cortex. When $I_{NaP}$ becomes activated at potentials positive to about −60 mV, it produces a gradual inward deviation of the current–voltage ($I/E$) relationship in these neurons, causing a point of zero slope conductance negative to the activation potential of the fast $I_{Na}$ (Stafstrom et al., 1982, 1985). Because $I_{NaP}$ sets the threshold for regenerative depolarization, it must play an important role in regulating neuronal excitability around firing threshold. While the transient and persistent $Na^+$ currents behave as functionally distinct conductances, it is still controversial whether they are mediated by two different populations of $Na^+$ channels with different gating kinetics or whether individual channels of a uniform population can switch between gating modes.

Immunocytochemically distinct $Na^+$ channel subtypes show a differential expression in several brain regions. Neuronal somata are rich in subtype RI, and axons are strongly immunoreactive for subtype RII (Westenbroek et al., 1989). Because $I_{NaP}$ appears to be predominantly generated at or near cell somata (Llinas and Sugimori, 1980), the differential spatial distribution of $Na^+$ channel subtypes led to the hypothesis that subtype RII would primarily mediate action potentials, whereas the somatic RI channels would generate $I_{NaP}$ (Westenbroek et al., 1989). On the other hand, recent studies of gating kinetics of single $Na^+$ and $Ca^{2+}$ channels have clearly demonstrated that individual channels can switch between two or more gating modes (Patlak and Ortiz, 1985, 1986; Kohlhardt et al., 1987; Nilius, 1988; Moorman et al., 1990; Plummer and Hess, 1991; Zhou et al., 1991; Ukomadu et al., 1992).

The present study was undertaken to elucidate the kinetics of $Na^+$ channel gating in mammalian cortical neurons and thus to determine the single-channel basis of the transient and persistent $Na^+$ currents. In order to perturb $Na^+$ channels as little as possible, initial experiments were performed in the cell-attached mode using the thin slice preparation. Later, single-channel recordings were also obtained from acutely isolated cortical cells.

Received May 15, 1992; revised July 31, 1992; accepted Aug. 10, 1992.

This work was supported by Office of Naval Research Grant N00014-90-J-1627, NINCDS grant NS 16792, and the W. M. Keck Foundation. C.A. is recipient of a research fellowship from the Deutsche Forschungsgemeinschaft (Al 294/2-1). We are grateful to Dr. Rod Sayer for his help with the cell dissociation procedure and to Drs. Albert Berger and Christine Livingston for their advice on the thin slice technique. We also thank Dr. Todd Scheuer for helpful discussions. Excellent technical assistance by Paul Newman and Gregg Hinz is gratefully acknowledged.

Correspondence should be addressed to Peter C. Schwindt, School of Medicine, Department of Physiology and Biophysics, SJ-40, University of Washington, Seattle, WA 98195.

In either preparation, we failed to observe two populations of $Na^+$ channels. Instead, individual channels from an apparently uniform population occasionally switched into a different gating mode in which they failed to inactivate for variable periods, producing a sustained burst of openings.

Some of these results have been published in abstract form (Alzheimer et al., 1992).

## Materials and Methods

*Acutely isolated neurons and thin slices.* Detailed accounts of slice preparations from rat and cat sensorimotor cortex have been published elsewhere (Stafstrom et al., 1984; Sayer et al., 1990). For experiments on acutely isolated neurons, 500-$\mu$m-thick slices were obtained from the dorsal frontoparietal (sensorimotor) cortex of young (10–21 d) or adult rats (2–5 months) and from the lateral cruciate region (architectonic area 4$\gamma$) of the neocortex of adult cats using a Vibratome or, in later experiments, a DSK microslicer. After dissection, slices were allowed to recover for about 1 hr in an interface-type chamber where they were constantly perfused with warmed (30–32°C) and gassed (95% $O_2$, 5% $CO_2$) artificial cerebrospinal fluid (ACSF; see Solutions and drugs, below). Slices were then transferred to warmed (28°C) HEPES-buffer saline (HBS; see below) saturated with $O_2$ to which 19 U/ml papain and 0.01 mM cysteine were added. After 90 min, slices were removed from the enzyme solution and washed in HBS. White matter was surgically removed, and the gray matter was cut into pieces 1–2 mm wide. The tissue pieces were maintained in HBS constantly bubbled with $O_2$ at room temperature (21–24°C) and remained viable for up to 7 hr. Before each recording session, a single piece of tissue was mechanically triturated using Pasteur pipettes of progressively decreasing tip diameter. To reduce cell damage, we used $Ca^{2+}$-free HBS that also contained 10 mM EGTA and 2 mM kynurenic acid. Immediately after dissociation, the cell suspension was transferred to the recording chamber where it was allowed to settle for about 7 min before gentle perfusion with HBS to remove floating debris. All recordings were performed at room temperature. The recording chamber was mounted either on the stage of an upright microscope (Zeiss) equipped with differential interference contrast (Nomarski) optics, which was also used for recordings from thin slices (see below), or on the stage of an inverted microscope (Nikon) equipped with phase contrast optics. The cells attached reasonably well to the glass bottom required for Nomarski optics although the plastic cell culture dishes (Falcon or Nunc) used for recordings on the inverted microscope proved superior in terms of cell attachment. The procedure of acute isolation worked well using animals 3 weeks or younger, but the yield of viable cells was much lower when adult animals were used.

The preparation and maintenance of thin slices as well as the recording configuration were similar to the procedures introduced by Edwards et al. (1989). Slices 120–150 $\mu$m thick were obtained from the sensorimotor cortex of 1–2 week old rats. After dissection, slices were placed into a lidded jar that contained warmed (34°C) and gassed (95% $O_2$, 5% $CO_2$) ACSF. After about 60 min, one slice was transferred to the recording chamber and the remaining slices were stored in a large holding chamber. Both chambers were perfused with gassed ACSF at room temperature. Thin slices were viable for 3–4 hr. Typical examples of pyramidal neurons in thin slices and after dissociation are illustrated in Figure 1.

*Recording conditions.* Single-channel recordings were obtained in the cell-attached or inside-out configuration of the patch-clamp technique as originally described by Hamill et al. (1981). In experiments from thin slices, visually identified layer V pyramidal neuron somata were cleaned from surrounding tissue by alternately applying positive or negative pressure through the broken tip of an HBS-filled microelectrode as outlined by Edwards et al. (1989). In later experiments, it was also possible to obtain single-channel recordings from superficially located cells without previous cleaning. For this purpose, positive pressure of about 10 cm $H_2O$ was applied through the tip of the recording electrode until it reached the membrane of the targeted cell. When working with acutely isolated cells, seal formation was always obtained while the cells were bathed in HBS. For some experiments, the bathing solution was then changed to a high $K^+$ solution to zero resting membrane potential (RMP), or to a $Ca^{2+}$-free, EGTA-containing solution used for patch excision (see Solutions and drugs, below).

The average lifetime of patches was usually between 10 and 30 min. Within the usual voltage range (−60 to −30 mV in high $K^+$ solution), less than about 25% of patches displayed significant $K^+$ channel activity. We did not, therefore, routinely add $K^+$ channel blockers to the microelectrode solution. Patches with interfering $K^+$ channel signals were excluded from analysis. The number of $Na^+$ channels in a patch (usually 4–12) was estimated by dividing the amplitude of the maximum overlap of channel openings by the single-channel amplitude. We assume that this calculation gives a low estimate of the true number of $Na^+$ channels in the patch because some channels may remain inactivated or fail to open at the potentials employed (Kunze et al., 1985; Kimitsuki et al., 1990b). In addition, as the number of active $Na^+$ channels in a patch exceeded five, screening for maximum number of overlapping openings became a less reliable method of counting channels (Aldrich et al., 1983).

*Single-channel recording and data analysis.* Microelectrodes were made from Corning glass (#7052) employing a two-stage pull protocol. The tapered region and the lowest part of the electrode shaft were coated with Sylgard. The tip was fire polished to give an electrode resistance of 4–8 MΩ when filled with standard electrode solution (see below). Single-channel currents were recorded and amplified using an Axopatch 1D. Before data acquisition, capacitive and leak currents were reduced by means of the built-in analog compensation circuits of the amplifier. Recordings were filtered at 1 or 2 kHz (−3 dB, 4 pole Bessel filter), digitized (TL-1 interface, Axon Instruments), and subsequently stored on hard disk. A single data file consisted of 150 repetitive voltage steps to a given test potential. The sampling rate depended on the length of the sweep, allowing 40 kHz during 50 msec sweeps and 5 kHz during 400 msec sweeps. The root mean square (RMS) noise was usually between 0.25 and 0.50 pA. Voltage pulse protocols were generated by a software program (pCLAMP 5.5, Axon Instruments), which was also used for data analysis. To improve signal-to-noise ratio, some recordings obtained at 2 kHz were digitally refiltered at 1–1.4 kHz. Whenever present, blank traces were summed up and the average was then subtracted from activity traces to nullify remaining capacitive and leak currents. A threshold crossing criterion equal to half the channel amplitude was employed to detect unitary channel activity. Lists of idealized channel events were created that were used for further analysis. Dwell time histograms and amplitude distributions were fitted by exponential and Gaussian curves, respectively, using a nonlinear, least-square fitting routine (Levenberg–Marquardt algorithm). Evaluation of fitting parameters was based on $\chi^2$ values and on the ratio between the number of calls to the $\chi^2$ subroutine and the number of iterations (goodness of fit). Open probability ($NP_o$) values of brief late openings were obtained by dividing the sum of brief late open times occurring after the decay of the peak ensemble current by the sum of the corresponding overall recording times. Values in the text are given as mean ± SEM unless otherwise stated.

To exclude the possibility that the application of 400 msec depolarizing pulses every 2 sec affected the frequency of occurrence of the brief late $Na^+$ channel openings described below, we computed their opening probability and mean open time during 400 msec pulses applied at either 0.2 or 0.5 Hz. No differences were found in these parameters at the lower repetition rate, nor did the incidence of late openings decrease during slow ramp depolarizations.

*Solutions and drugs.* ACSF contained (in mM) NaCl, 130; KCl, 3; $CaCl_2$, 2; $MgCl_2$, 2; $NaH_2PO_4$, 1.25; $NaHCO_3$, 26; D-glucose, 10 (pH 7.4). The composition of HBS was identical to the above solution except that bicarbonate was replaced by 25 mM HEPES/Na-HEPES. High $K^+$ saline consisted of (in mM) K-aspartate, 136; $MgCl_2$, 5; HEPES, 25; D-glucose, 10 (pH 7.4). Inside-out patches were obtained in one of the following solutions (in mM): (1) methanesulfonic acid, 79; K-aspartate, 50; NaCl, 4; $MgCl_2$, 1; EGTA, 9; HEPES, 8 (pH 7.2–7.3 adjusted with CsOH); or (2) CsF, 125; NaCl, 4; $MgCl_2$, 1; EGTA, 9; HEPES, 8 (pH 7.2 adjusted with CsOH). Both solutions yielded comparable results. The standard microelectrode solution consisted of (in mM) NaCl, 123; KCl, 3; $CaCl_2$, 2; $MgCl_2$, 2; $NaH_2PO_4$, 1.25; HEPES/Na-HEPES, 14 (pH 7.4). Lidocaine was obtained from Sigma.

## Results

To evoke single $Na^+$ channel currents, depolarizing test pulses of varying amplitudes were applied to membrane patches that were held 40–60 mV negative to RMP in normal saline and at −100 mV in high $K^+$ solution. The length of the test pulse was varied between 50 msec and 400 msec in order to resolve early openings and late events, respectively. Almost every patch contained $Na^+$ channels that were identified by current polarity,

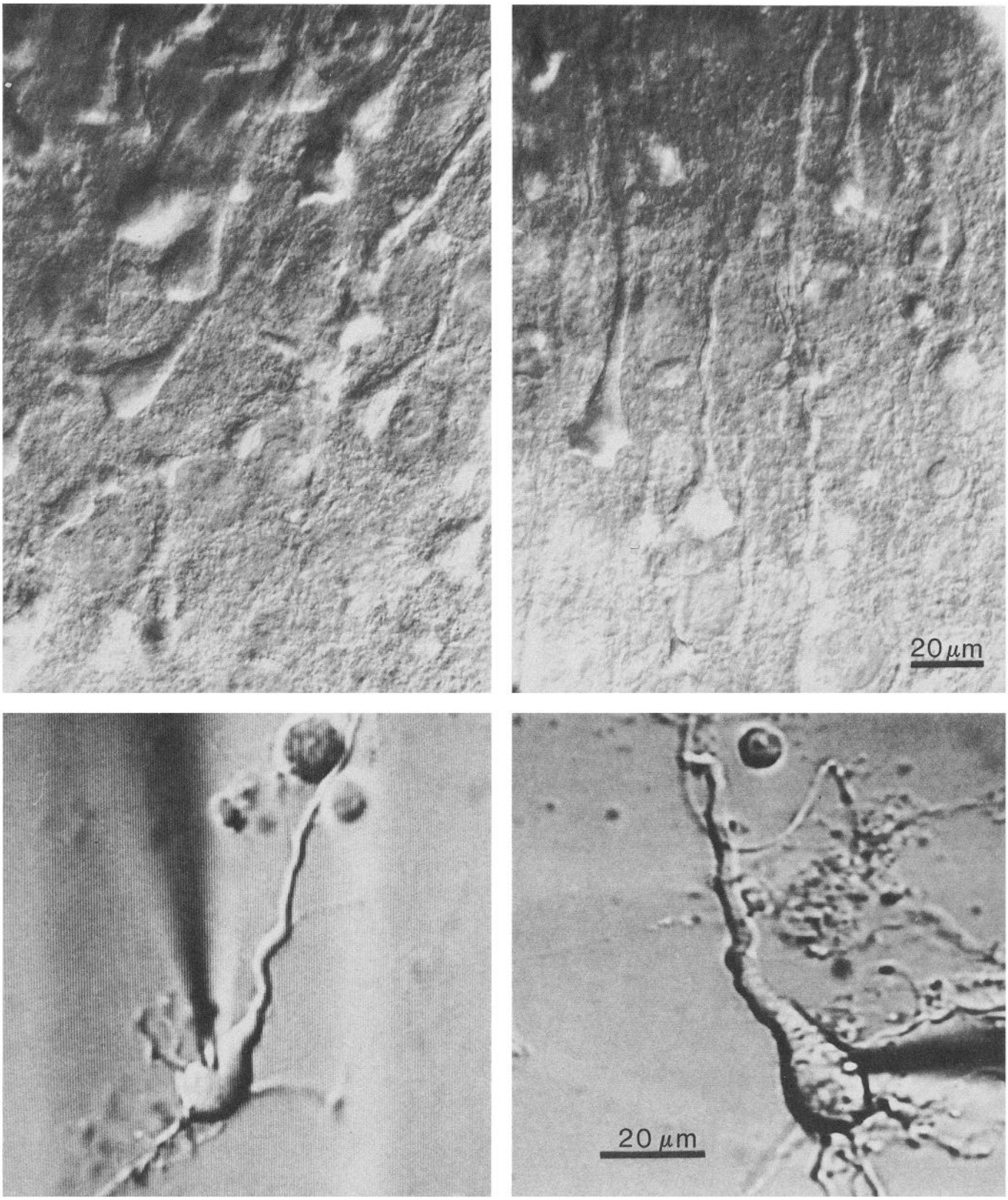


*Figure 1.* Preparations and cell morphology. The *top panels* show layer V neurons in a thin neocortex slice (130 μm) from a 10-d-old rat. The photographs were obtained by means of Nomarski optics using a water immersion objective. The *bottom panels* depict two acutely isolated pyramidal neurons from the same brain region obtained from a 10-d-old rat (*left*) and a 14-d-old rat (*right*). Recording electrodes are attached to the somata of the dissociated cells, which were photographed from the stage of an inverted microscope using Hoffman optics.

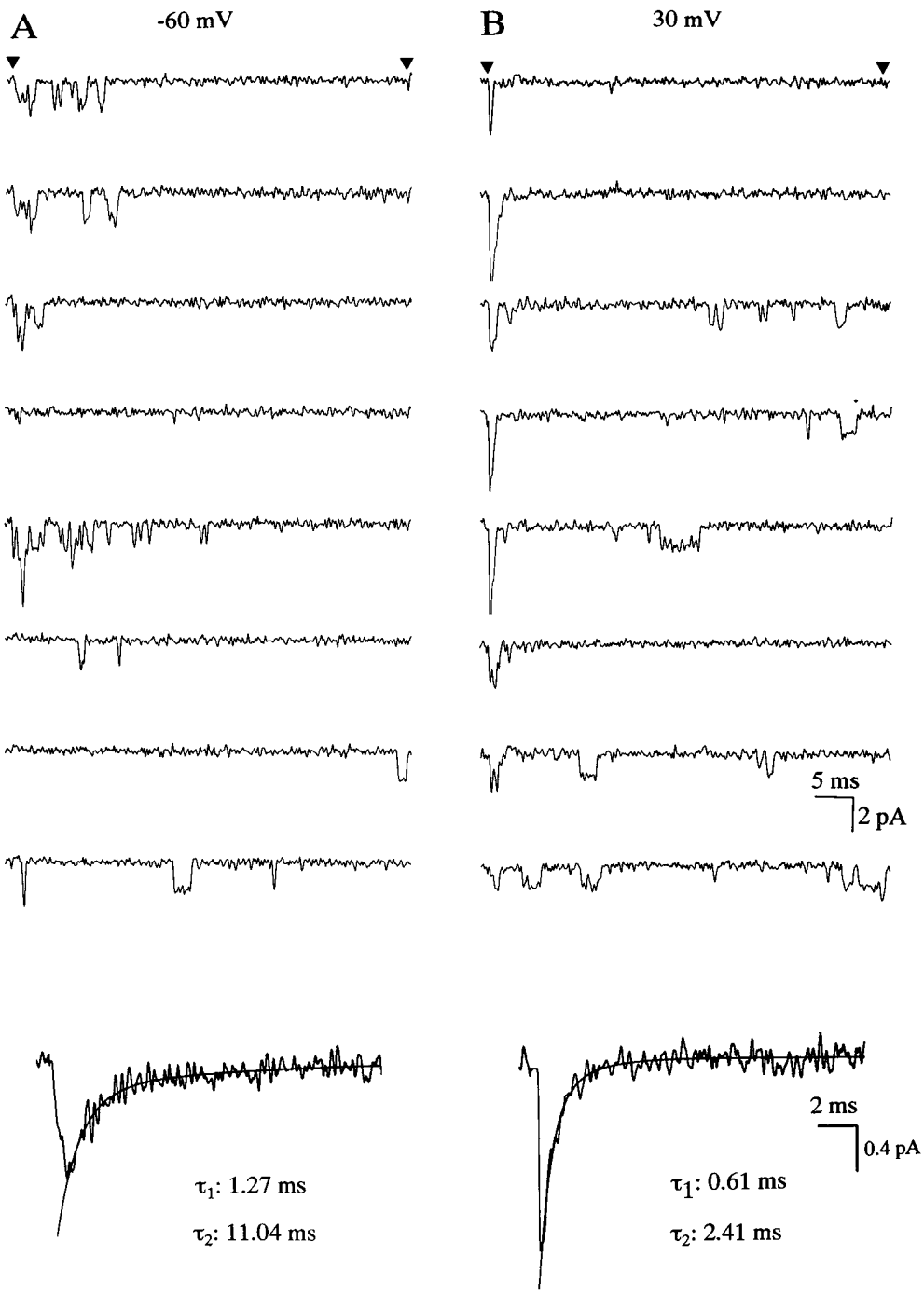


*Figure 2.* Early transient openings of $Na^+$ channels: cell-attached recordings from a dissociated neuron that was superfused with a high $K^+$ solution. $V_H$ was −100 mV. *Triangles above top traces* indicate duration of depolarizing voltage step to −60 mV (*A*) and −30 mV (*B*). Representative single traces were selected from an ensemble of 150 sweeps. Ensemble average currents are shown below single sweeps. Note that ensemble currents are depicted on faster time scale to better resolve time course of inactivation. For further explanation, see text.

unitary current amplitude, and voltage-dependent gating. In addition, $Na^+$ channel openings were not blocked by external cadmium (0.4 mM added to pipette solution), but were completely and reversibly blocked by lidocaine (40 μM added to the bath; data not shown). No patches contained only one $Na^+$ channel. Patches from young animals contained 4–12 $Na^+$ channels; in older animals we observed patches with up to approximately 20 or more channels. In addition to the expected early transient $Na^+$ channel openings, we observed late channel activity consisting of brief late openings and bursts of sustained activity during a maintained depolarization. Because our prime interest was in the possible mechanism of $I_{NaP}$, our study focused on the late activity. We treated all channel data from thin slices and acutely isolated cells as a homogeneous set since the channel activity observed in each preparation was identical.

*Early transient openings*

Figure 2 shows inward channel currents at two test potentials on a fast time scale. At a test potential of −60 mV (Fig. 2*A*), the latency to the first opening was widely distributed over the entire trace so that channel openings rarely overlapped at the beginning of the pulse. In addition, channels occasionally went through a period of repetitive reopenings before they eventually inactivated. In contrast, at a test potential of −30 mV (Fig. 2*B*) the first openings were clustered immediately after the onset of the pulse. These openings displayed a high degree of synchronization and a decreased likelihood of repetitive reopenings. Channel behavior at each potential is reflected in the ensemble average currents shown below the single-channel traces (Fig. 2). As the test potential was made more positive, the peak current

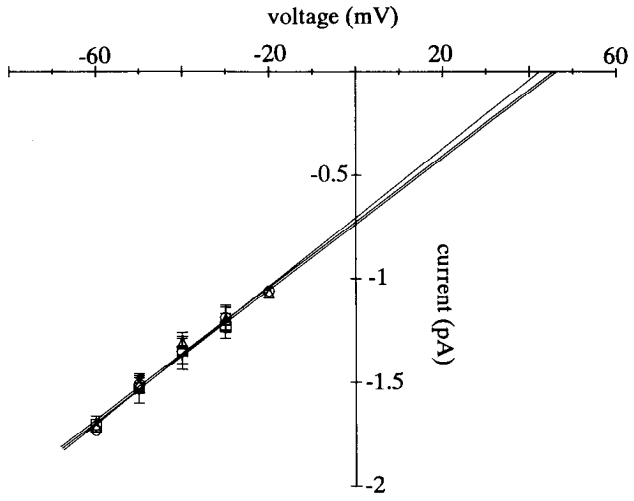


*Figure 3.* Current–voltage relationships of $Na^+$ channels mediating early and late activity. Unitary amplitudes were determined from cell-attached recordings from dissociated neurons bathed in high $K^+$ saline. Since $Na^+$ channel openings were often too short to be fully resolved, traces were screened for long square openings that allowed unequivocal measurements of amplitude. For the construction of single-channel *E* curves, mean amplitude values from 2–19 independent recordings at a given test potential were averaged and plotted as mean ± SD. Error bars are not shown when smaller than symbol size or when only two amplitude values were available. *I/E* curves were obtained by linear regression. $Na^+$ channels mediating early transient openings (*triangles*) had a slope conductance of 15.9 pS ($r = 0.99$) and an extrapolated reversal potential of 46 mV. $Na^+$ channels mediating brief late openings (*circles*) had a slope conductance of 16.6 pS ($r = 0.99$) and an extrapolated reversal potential of 42 mV. Noninactivating $Na^+$ channels (*squares*) had a slope conductance of 15.9 pS ($r = 0.99$) and an extrapolated reversal potential of 46 mV.

became substantially larger but inactivated faster. The decay of the ensemble current was best fitted with two time constants in agreement with previous results from whole-cell recordings in the same preparation (Huguenard et al., 1988).

The slope conductance of inward channel currents was determined by plotting unitary current amplitude as a function of test potential. Figure 3 summarizes the current–voltage (*I/E*) relationship of early transient openings (triangles). For comparison, the figure also contains the *I/E* relations of the brief late openings (circles) and sustained bursts (squares) that will be described below. In all cases, the inward channels displayed a linear *I/E* relationship within the voltage range tested. The extrapolated reversal potential ranged between 42 and 46 mV. Unitary current amplitude at −50 mV was about −1.5 pA. Slope conductance varied between 15.9 and 16.6 pS and was within the range of other vertebrate $Na^+$ channels (Neumcke, 1990). Thus, both the early and late channel currents described in this article were mediated by a population of $Na^+$ channels that have uniform elementary electrophysiological properties.

### *Brief late openings*

In addition to the transient, rapidly inactivating openings, Figure 2 reveals an additional gating phenomenon of $Na^+$ channels; namely, $Na^+$ channels displayed brief late openings during sustained depolarization. The time course of the ensemble current (Fig. 2, bottom) indicates that inactivation was complete within few milliseconds. Nevertheless, isolated or repetitive late openings were observed at variable times after the early openings. This is most evident in the recordings obtained at −30 mV (Fig. 2*B*).

In order to study the brief late openings in more detail, we employed depolarizations lasting 400 msec. A representative example of this set of experiments is illustrated in Figure 4, which shows early and late openings at three different test potentials. Brief late openings occurred as single or multiple events, sometimes clustered in "minibursts" lasting up to 40 msec. Visual inspection of Figure 4 suggests that the gating of the brief late openings was voltage dependent. This impression was confirmed by calculating the mean open time and the open probability of the late events as a function of test potential. These calculations were based on the assumptions (1) that all channels in the patch were homogeneous kinetically and had the same probability of reentering the open state, and (2) that the number of active channels remained constant during recording. For reasons explained in Materials and Methods, we could estimate only the minimum number of $Na^+$ channels in the patch. Thus, open probabilities are given as $NP_o$ values. The very low incidence of brief late openings ($NP_o \ll 0.01$; see below) yielded only a limited number of data points. Nevertheless, open time histograms could be fitted reasonably well by a single exponential curve (Fig. 4, bottom). Within the voltage range tested (−60 to −20 mV), the mean open times of the brief late openings varied between 0.2 and 0.6 msec and showed a moderate, bell-shaped voltage dependence with a maximum around −40 mV (Fig. 5*A*). A similar voltage dependence has been observed for transient $Na^+$ channel openings in several preparations (see Discussion). The decay of mean open times at potentials positive to −40 mV should be regarded with some caution since we cannot rule out that the decreased signal-to-noise ratio at these potentials might have biased our measurements towards artifactually shorter dwell times in the open state. $NP_o$ values displayed a voltage dependence similar to that of mean open times, although the peak value was shifted about 10 mV in the depolarizing direction (Fig. 5*B*). This voltage dependence also was evident during slow voltage ramps. In these experiments, the patches were depolarized from −80 to −20 mV over 1 sec, and the incidence of late openings was counted as a function of the voltage where they occurred. Data from two patches where such voltage ramps were employed are shown in Figure 5*C*. These data also support the idea that late openings are present throughout a wide voltage range but have the highest incidence between −40 and −20 mV.

Brief late openings occurred infrequently, but they were observed consistently in all patches. As revealed by "diaries" of late activity (not shown), which were reconstructed from eight different recordings, brief late events were quite evenly distributed over the entire recording period with at least one brief event present in 61.6 ± 5.4% of all sweeps. Repetitive brief openings ("minibursts") were observed in 36.0 ± 5.2% of all traces containing brief late activity. Sometimes, "minibursts" occurred in three or four consecutive sweeps. This clustering suggests that one $Na^+$ channel in the patch might have undergone a temporary transition allowing repetitive reopenings. However, due to the multichannel nature of our recordings, we cannot provide direct evidence for this inference. At test potentials between −60 and −40 mV, where the frequency of brief late openings did not display an appreciable voltage dependence (Fig. 5*B*), we calculated an average $NP_o$ value of 0.0034 ± 0.0021 (range, 0.00032–0.0089; $n = 23$ patches). The incidence of these events may be higher in adult animals. We succeeded

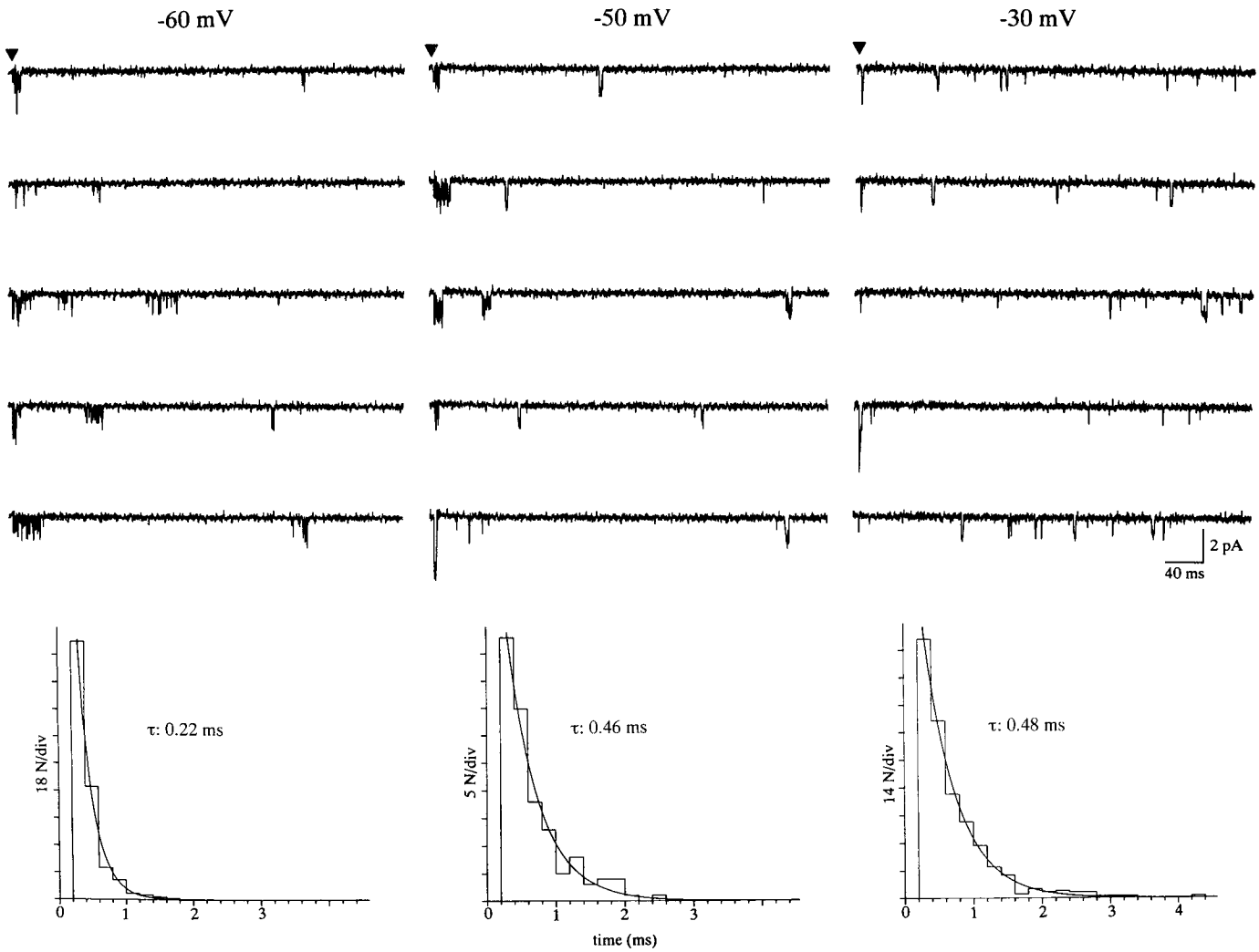


*Figure 4.* Phenomenology and open time histograms of brief late openings. Cell-attached recordings were obtained from an acutely isolated neuron superfused with high $K^+$ saline. For illustration, traces were selected for late activity. *Triangles above top traces* indicate onset of depolarizing voltage steps. Open time histograms are shown below the corresponding single-channel traces. They include all brief late openings that occurred during 150 consecutive voltage steps to a given test potential. Histograms were best fitted by a single exponential.

in obtaining sufficient data from two mature pyramidal cells to calculate $NP_o$ values. These values (0.011 and 0.023) were about one order of magnitude higher than in the young rats. Unfortunately, pyramidal neurons from adult animals rarely survived the dissociation procedure.

*Sustained bursting activity*

In addition to the brief late openings, we found another mechanism for sustained $Na^+$ influx during prolonged depolarization, namely, occasional failure of $Na^+$ channel inactivation. A typical example of an inactivation failure is contained in Figure 6*A*. These records are from a cell-attached recording from an identified layer V pyramidal cell in a thin slice. In all but one trace, $Na^+$ channels inactivated rapidly and occasionally displayed brief late openings. In the third trace from bottom, however, a single $Na^+$ channel in the patch failed to inactivate and produced a sustained burst of openings. Often, the burst persisted for the entire depolarization, but bursts also ceased spontaneously during maintained depolarization (e.g., see Fig. 8*A*, top trace). To be included in our analysis, a sustained burst had to last longer than 80 msec, which was twice the time of the longest "minibursts" (see above). This distinction between repetitive brief late openings and sustained bursts was supported by the fact that almost no bursts were observed to last between 40 and 80 msec.

A single $Na^+$ channel in a patch entering the bursting mode was observed in 1.1 ± 0.2% of all depolarizations ($n$ = 34 patches). Failures of inactivation occurred at all test potentials examined (−60 to −10 mV). Due to the rare incidence of sustained bursts and limited recording time, we were not able to gather sufficient data to investigate statistically a possible voltage dependence of this gating shift. However, a comparison of six patches where we recorded sustained bursts at two test potentials (−50 and −30 mV) suggested that failure of inactivation had only a very moderate voltage dependence, if any. At −50 mV, noninactivating $Na^+$ channels were observed during 0.62 ± 0.07% of the depolarizations, whereas this behavior occurred during 0.85 ± 0.15% of the depolarizations to −30 mV.

A kinetic analysis of gating during a sustained burst is shown in Figure 6, *C* and *D*. The histograms were obtained from the bursting sequence shown above at high magnification (Fig. 6*B*). Both the closed time histogram (Fig. $6C_1$) and the open time histogram (Fig. $6C_2$) were fitted best by a single exponential

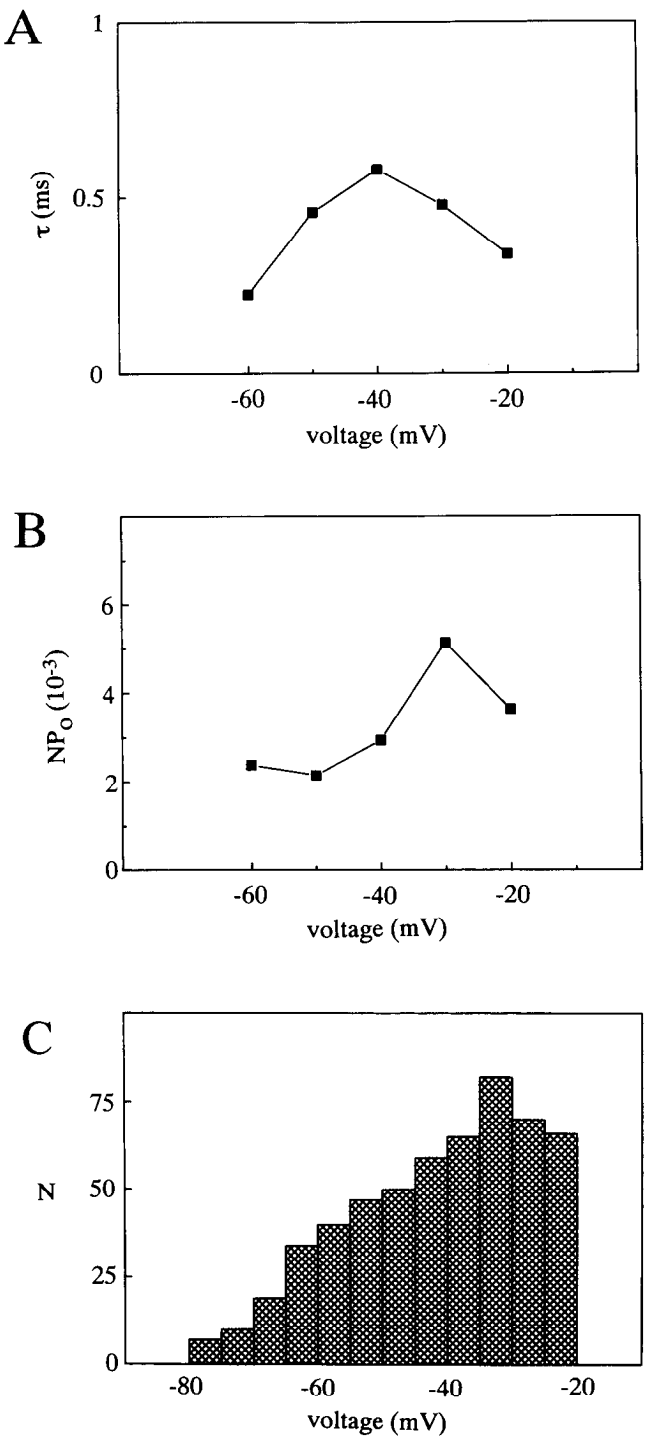


*Figure 5.* Voltage dependence of brief late openings. *A* and *B*, Mean open time ($\tau$) and open probability ($NP_o$) are plotted as a function of test potential. Data were obtained from same patch as in Figure 4. *C*, Using slow depolarizing voltage ramps, as illustrated in Figure 9, the incidence of brief late openings was related to the voltage where they occurred. For this purpose, voltage ramps were binned into 5 mV segments, and the number of observations ($N$) was counted within each bin.

curve yielding mean closed and open times of 0.53 and 2.34 msec, respectively. Although only a limited number of data points were available for calculation, the amplitude histogram of the open level was fairly well described as a single Gaussian distribution (Fig. 6*D*).

In recordings from 1–3-week-old rat neocortex, sustained bursts were almost always confined to a single depolarization. In an acutely isolated neuron from adult cat neocortex, however, we observed noninactivating $Na^+$ channel gating that extended over four consecutive 400 msec depolarizations delivered every 2 sec (Fig. 7*A*). No channel activity was seen during the intermittent repolarizations. Since the patch had more than one $Na^+$ channel, we cannot completely exclude the possibility that independent bursts of several $Na^+$ channels were clustered, giving the impression of a particular channel entering a long-lived bursting mode. However, this is unlikely in view of the rare incidence of inactivation failures (see above). Hence, the kinetic analysis of the burst was performed assuming that the whole sequence was mediated by a single channel. A mean open time of 0.5 msec was calculated from the open time histogram (Fig. 7*B*, top). In contrast to the burst illustrated in the previous figure, the closed time histogram was fitted best with two exponentials giving time constants of 0.3 and 1.2 msec (Fig. 7*B*, bottom), suggesting that this channel entered a single open state from two different nonconductive states.

Mean open times during sustained bursts were voltage dependent. An example is shown in Figure 8*A*, which depicts bursting activity recorded from the same patch at two test potentials. Since the patch, as always, contained several $Na^+$ channels, the two bursts might be mediated by different $Na^+$ channels. In Figure 8*B*, mean open times obtained from several experiments are plotted as a function of test potential. Although mean open times could vary widely at a given potential, there was a clear tendency for a bursting $Na^+$ channel to stay open longer at more depolarized potentials. The average fractional open time of $Na^+$ channels during a burst at $-50$ mV was 0.47 $\pm$ 0.10 ($n$ = 5).

Single-electrode voltage-clamp experiments on cat cortical pyramidal neurons have shown that a depolarizing voltage ramp evoked a persistent $Na^+$ current prior to and independent of the activation of the fast $Na^+$ current (Stafstrom ct al., 1982, 1985). If the $Na^+$ channel bursts observed during voltage steps were the predominant mechanism underlying $I_{NaP}$, they should also occur during slow voltage ramps that did not elicit transient openings. The experiments illustrated in Figure 9 show that the single-channel kinetics indeed paralleled the behavior of the whole-cell current. In order to apply a slow voltage ramp, the sampling rate had to be reduced to 2 kHz. Therefore, $Na^+$ channel openings, especially those occurring at more negative potentials where the open time was shortest, were not always fully resolved. Similar to their incidence after voltage steps, noninactivating $Na^+$ channels were observed in 1.8 $\pm$ 1.2% of all depolarizing voltage ramps ($n$ = 3 patches). Two examples of sustained bursts during voltage ramps are illustrated in Figure 9. The fractional open time during the bursts increased substantially as the membrane potential became more positive, supporting the previous notion (Fig. 8) that burst kinetics were voltage dependent. In addition, the two burst sequences in Figure 9 confirm the implication drawn from Figure 8*B*, namely, that within a certain voltage-dependent framework, individual channels can display a considerable degree of freedom in their gating behavior. For example, the burst illustrated in Figure 9 (left panel) began with brief, widely spaced openings followed by frequent transitions between open and closed states as the patch was depolarized further. Although the burst shown in the right panel of Figure 9 developed at about the same potential, its characteristics were quite different. After an initial series of

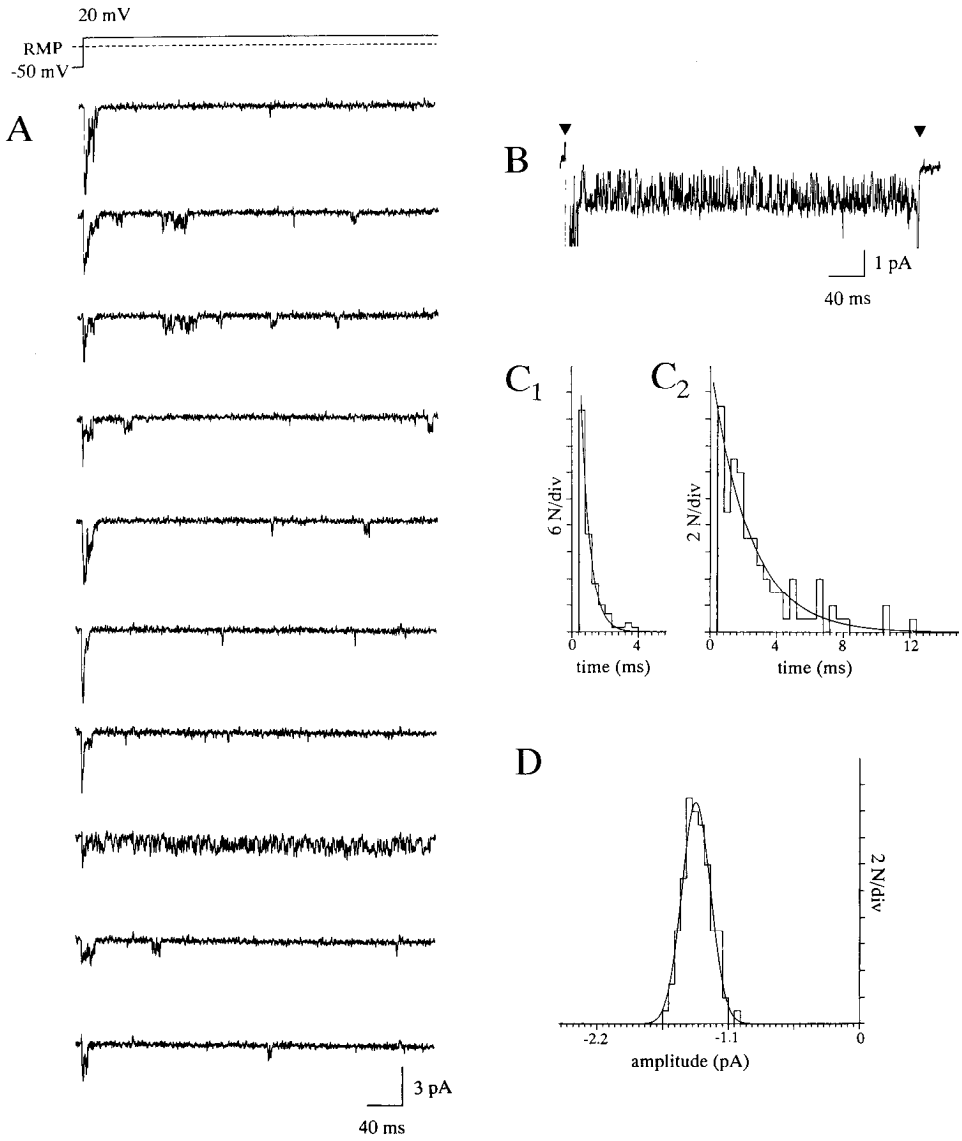


*Figure 6.* Occasional failure of $Na^+$ channel inactivation. *A*, Cell-attached recordings from a visually identified layer V pyramidal neuron in a thin slice from rat cortex. The slice was superfused with ACSF. Brief late openings were sometimes clustered in "mini-bursts" lasting up to 40 msec. Note failure of inactivation in third trace from bottom causing a sustained burst of activity. *B*, Persistent burst of openings recorded from another patch and shown at higher magnification (dissociated cell, high $K^+$ saline, $V_H$ −100 mV, $V_T$ −50 mV). Overlapping early transient openings after onset of voltage step are truncated. *C*, Closed ($C_1$) and open ($C_2$) time histograms of $Na^+$ channel during the bursting activity shown above. Time constants were 0.53 msec and 2.34 msec, respectively. *D*, Amplitude histogram of open level from same burst.

brief openings and closures, the channel spent most of its time in the open state, only occasionally occupying a nonconductive state. The $Na^+$ channels mediating the bursts had slope conductances of 15.8 and 15.9 pS; the extrapolated reversal potentials were 52 and 45 mV, respectively.

*Inside-out recordings*

In the last set of experiments, we investigated the hypothesis that sustained bursts might require the presence of a diffusible cytosolic substance. For this purpose, we performed a series of inside-out recordings. Five inside-out patches were obtained from dissociated cells, one from a neuron in a thin slice. Prior to patch excision, the bathing medium was switched to a $Ca^{2+}$-free solution. After excision, activation and inactivation of $Na^+$ channels were shifted by about 20–40 mV in the depolarizing direction. Patch excision has been found to impair inactivation in some preparations (for review, see Neumcke, 1990). In our recordings, however, impaired inactivation was observed only in one patch that was discarded from subsequent analysis. Persistence of normal $Na^+$ channel gating after patch excision was also observed in nonpyramidal cortical cells maintained in culture (Kirsch and Brown, 1989). As shown in Figure 10, $Na^+$ channels usually retained their regular gating kinetics with both the brief late openings and the sustained bursts. The brief late openings had a mean open time of 0.47 ± 0.04 msec ($n$ = 5) and $NP_o$ values ranged between 0.001 and 0.002 (mean = 0.0017; $n$ = 5). Sustained bursts were observed in 0.7% of all depolarizations (range, 0.4–1.0%). Interestingly, in two excised patches we also recorded sustained bursts of inward current having about one-third the unitary amplitude of $Na^+$ channels. An example is illustrated in Figure 10 (left panel, third trace from top). This gating behavior was very similar to that of regular $Na^+$ channels, suggesting that, for some reason, the openings of an $Na^+$ channel in the patch were temporarily confined to a subconductance level. Since we observed these low-conductance bursts only in excised patches, it is possible that patch excision might have favored a transition to a subconductance state. We cannot completely exclude the presence of a second population of $Na^+$ channels, but the extremely rare incidence of these events indicates that neither a subconductance level nor a second population of $Na^+$ channels should contribute more than a negligible amount to the whole-cell current.

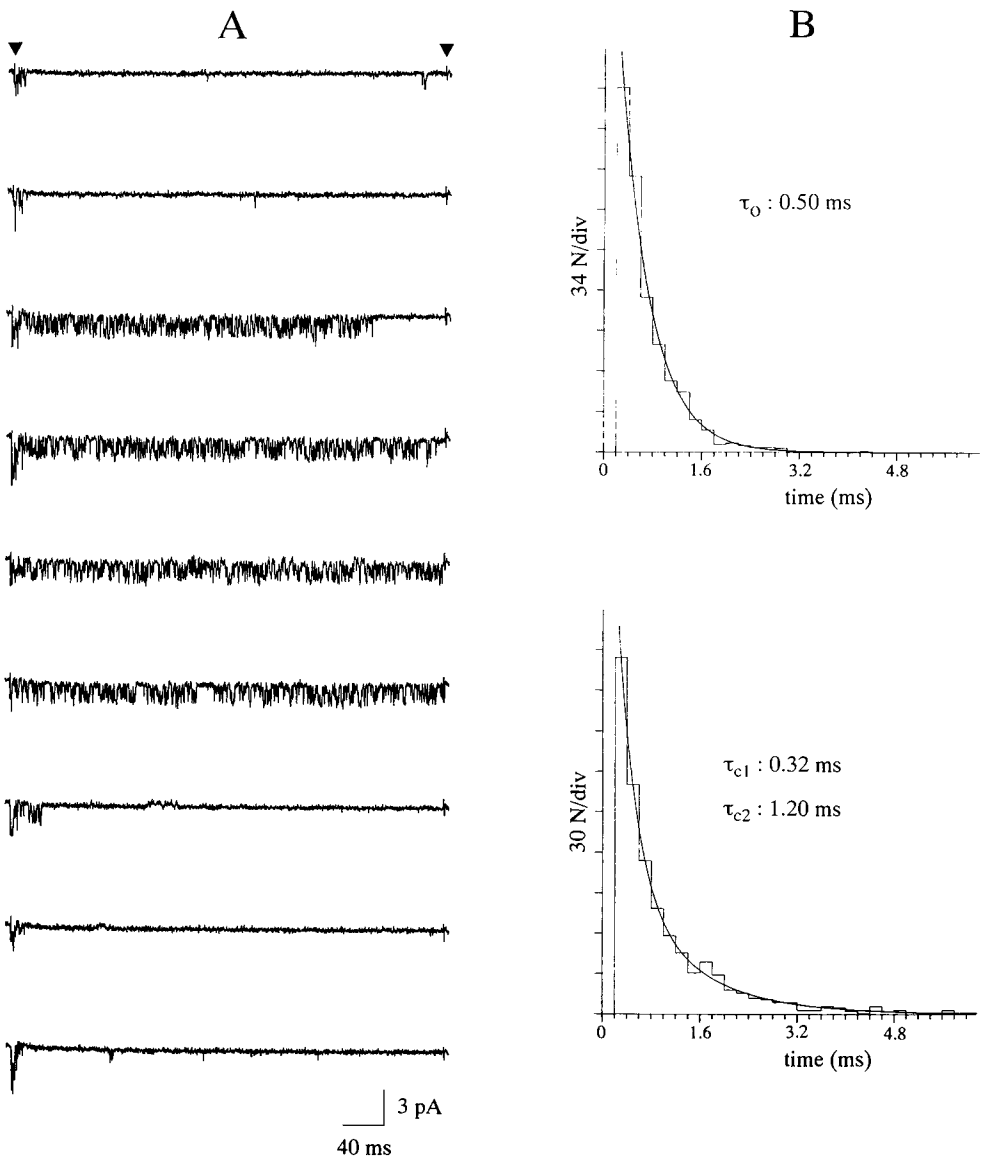


*Figure 7.* Failures of $Na^+$ channel inactivation during consecutive depolarizations in a dissociated neuron from cat neocortex. *A* shows nine consecutive cell-attached recordings obtained from an acutely isolated pyramidal neuron from adult cat sensorimotor cortex (high $K^+$ saline, $V_H$ −100 mV, $V_T$ −60 mV). *B*, Open (*upper*) and closed (*lower*) time histograms of $Na^+$ channel gating during the bursting activity in *A*. For explanation, see text.

## Discussion

*Late $Na^+$ channel gating occurs in two modes*

Our data indicate that $Na^+$ channels on the somata of neocortical pyramidal cells exhibit late activity during prolonged depolarization in addition to the transient, rapidly inactivating openings that underlie the upstroke of the action potential. Late channel openings were found to occur as (1) background activity consisting of sporadic brief openings with apparently intact inactivation and (2) as sustained bursts of openings caused by a temporary loss of inactivation. Comparing early openings, brief late openings, and sustained bursts, we failed to detect any significant difference in the elementary electrophysiological properties of the channels mediating these events. Both unitary amplitude and slope conductance were almost identical (Fig. 3). It thus appears that we recorded an electrophysiologically uniform population of $Na^+$ channels that can individually convert between gating modes rather than from two or more populations of ion channels endowed with different gating kinetics. Due to limitations inherent to our experimental approach, we cannot, however, provide final evidence for this conclusion. Based on immunocytochemical findings, it is likely that we recorded from more than one $Na^+$ channel subtype. Although the RI subtype prevails in adult neuron somata, we might have encountered the RII subtype occasionally and, especially in young animals, the RIII subtype (Westenbroek et al., 1989). Our data suggest, however, that immunocytochemical variations do not necessarily imply a difference in electrophysiological functioning. Since we never recorded from a patch containing only one active $Na^+$ channel, we cannot rule out the possibility that sustained bursting was produced by a second population of $Na^+$ channels. However, recent studies have shown that individual $Na^+$ channels expressed from a single clone can switch between gating modes as described here. In single-channel recordings, cloned RIII and $\mu$I $Na^+$ channel subtypes occasionally failed to inactivate and entered a prolonged bursting mode (Moorman et al., 1990; Zhou et al., 1991; de Leon et al., 1992; Ukomadu et al., 1992). Hence, we are confident that the observations made in our preparation were due to similar gating shifts. Since we observed sustained bursts both in dissociated cells and in neurons from thin slices, it can also be excluded that the occasional failure of inactivation was an artifact due to the dissociation procedure.

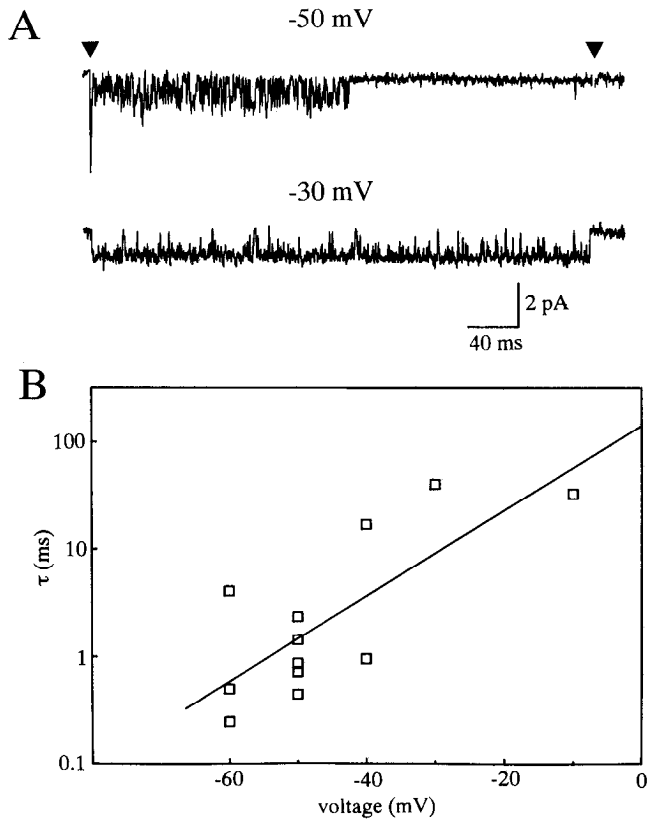


*Figure 8.* Voltage dependence of gating kinetics during bursts. *A*, Bursts of $Na^+$ channel openings recorded at two different test potentials from same patch (cell-attached recording from a dissociated cell, high $K^+$ saline, $V_H$ −100 mV). *B*, Mean open times during bursts were plotted as a function of test potential. Each data point represents mean open time of a single sustained burst. All data were obtained from cell-attached recordings from neurons bathed in high $K^+$ solution. For this analysis, only those bursts lasting the entire depolarizing steps were used. Bursts were also selected for low RMS noise levels. *Solid line* was determined by linear regression ($r = 0.77$).

Our data from inside-out patches indicate that late gating did not require cytoskeletal support or the presence of cytosolic factors. In fact, the incidence of brief late openings and occasional failures of inactivation remained almost unchanged after patch excision (Fig. 10), suggesting that the bursting mode is a property of the channel and/or adjacent membrane-bound structures (cf. Moorman et al., 1990). On the other hand, Ono and Fozzard (1991) reported that cAMP-dependent phosphorylation can modify late current through cardiac $Na^+$ channels. As evidence accumulates that phosphorylation of brain $Na^+$ channels alters fast gating (Dascal and Lotan, 1991; Numann et al., 1991; for review, see Catterall, 1988), it is conceivable that late $Na^+$ channel gating in neurons will emerge as a target of neuromodulation.

### *Kinetics of late $Na^+$ channel gating*

Within the limitations of our recording conditions, we attempted to gain some insight into possible kinetic schemes underlying late activity. Considering the brief late openings, the mean open time of these events displayed a moderate, bell-shaped voltage dependence reaching a maximum around −40 mV (Fig. 5*A*). Transient $Na^+$ channel openings exhibit a similar voltage dependence in several preparations (Sigworth and Neher, 1980; Horn et al., 1984; Barres et al., 1989; Scanley et al., 1990; Lawrence et al., 1991; but see Aldrich and Stevens, 1987). The kinetics of brief late openings should be very similar to those of transient openings if $Na^+$ channel kinetics can be described as a time-homogeneous Markovian process where the rate constants depend only on the present voltage, and where occasional reentries from inactivated to open states are allowed. According to this scheme, once a channel has reentered the open state from the inactivated state, its immediate future would be indistinguishable from that of a channel previously in a closed state. This scheme cannot account for the quantitative behavior of the brief late openings, however. At a test potential of −30 mV, for example (Figs. 2*B*; 4, right panel), the early transient open-

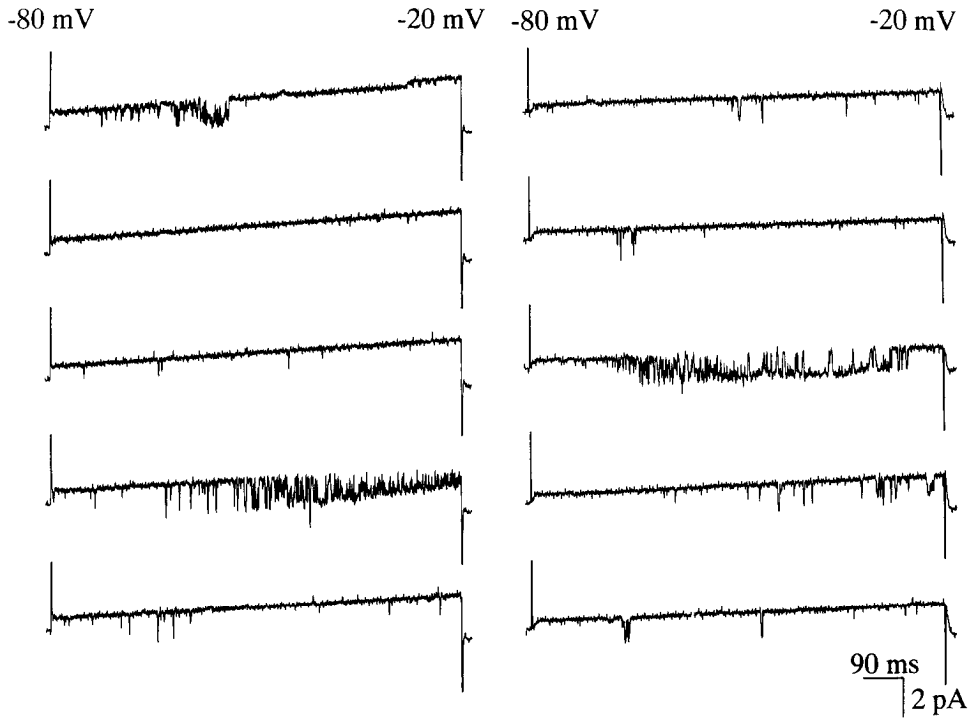


*Figure 9.* $Na^+$ channel gating during slow voltage ramps. Cell-attached patches from two dissociated cells bathed in high $K^+$ solution were gradually depolarized by means of a slow voltage ramp. Leak and capacitive currents were not subtracted. Single traces were selected for activity.

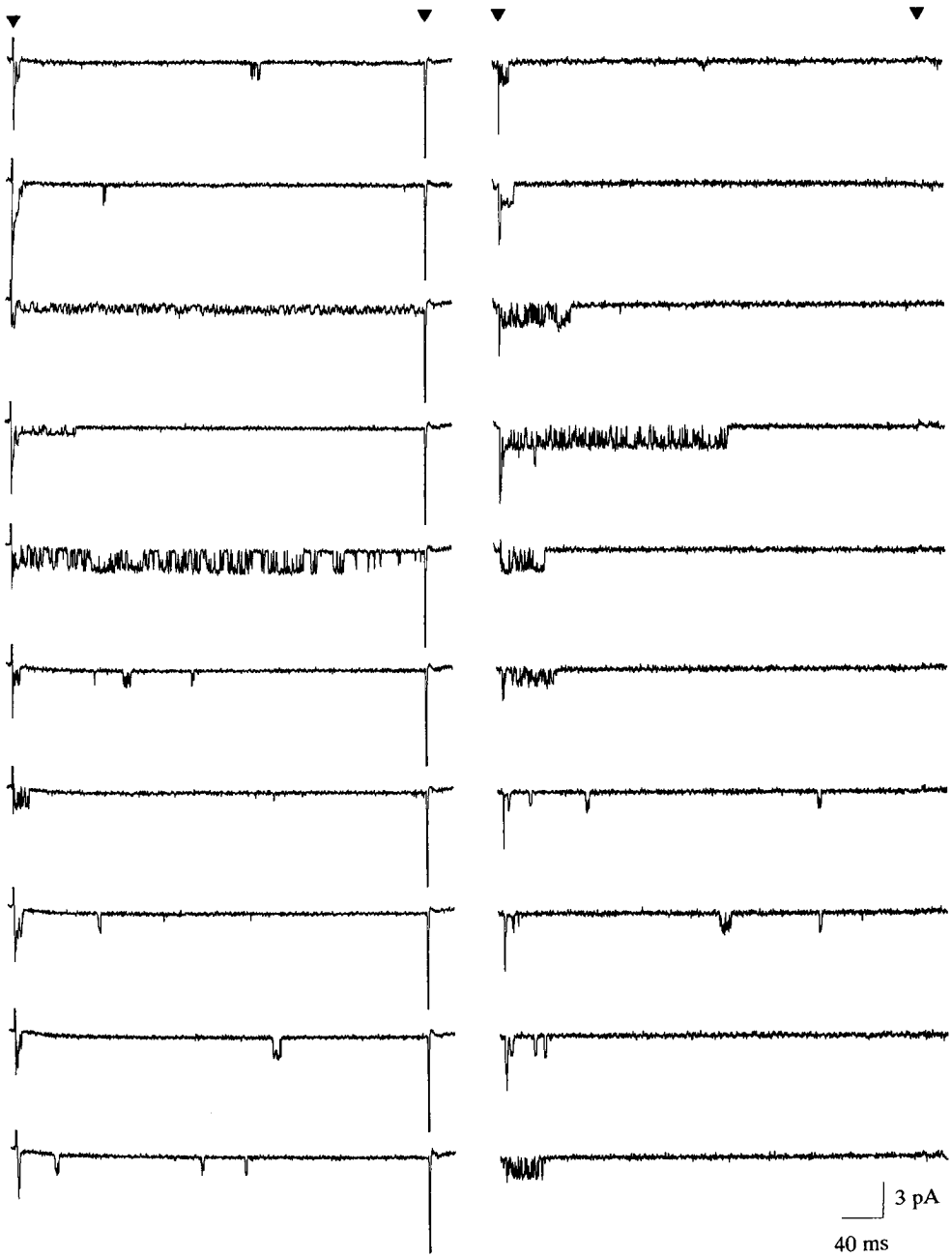


*Figure 10.* Inside-out recordings from two excised patches. After patch excision in Ca-free solution, activation and inactivation of $Na^+$ channels were shifted by about 20–40 mV in the depolarizing direction ($V_H$ −60 mV, *left*, and −80 mV, *right*; $V_T$ 0 mV). Nevertheless, the pattern of early and late gating remained substantially unchanged. Note the sustained burst of low-conductance openings in the *third trace from top in the left panel*, which also is present at the beginning of the next step.

ings were much shorter than the late openings. Possibly one or more of the rate constants controlling the open dwell time undergo some change during sustained depolarization, or the channel may have more than one open state.

While we can explain brief late openings within the usual framework of $Na^+$ channel kinetics, the occurrence of sustained bursts requires a substantial alteration in normal gating. Mean open time during sustained bursts increases with depolarization. This behavior contrasts with the bell-shaped voltage dependence of brief late openings and is reminiscent of $Na^+$ channels in which inactivation was removed chemically (Horn et al., 1984; Quandt, 1987). Hence, the simplest explanation of the sustained bursts is a temporary blockade of the transition to an inactivated state. The kinetics during bursting would then be controlled only by the remaining activation/deactivation gates. For example, a kinetic analysis of the burst shown in Figure 6*B* suggested that this channel made rapid transitions between one open and one nonconductive state, which would likely be a closed state. We also observed bursts where the channel could enter two nonconductive states, as indicated by a double exponential fit of the closed time distributions (Fig. 7*B*). In this case, one might assume that the channel made transitions between an open state, a closed state, and a less absorbing, inactivated state.

Patlak and Ortiz (1989) provided strong evidence that $Na^+$ channel openings during sustained bursts displayed a degree of kinetic diversity that was inconsistent with the standard time-homogeneous Markovian chain model. Instead, rate constants had to be quite flexible, even within short time spans, to allow the variety of burst phenomena observed. Our data support this notion in two ways: (1) the number of states entered during a burst appeared to be variable (see above), and (2) there was considerable variation at a given voltage (Fig. 8). Thus, the temporary loss of inactivation might result from several con-

formational changes, each producing somewhat different burst kinetics.

*Can late $Na^+$ channel gating result in a functional $Na^+$ current?*

In view of the low incidence of brief late openings and sustained bursts, one might question whether these features of $Na^+$ channel gating suffice to generate a physiologically significant whole-cell current. The magnitude of such a current is given by the product of the number of channels mediating the current ($n$) times their open probability ($p$) times the unitary current ($i$). Since both brief late openings and sustained bursts contribute, the persistent sodium current ($I_{NaP}$) can be described by the following equation:

$$I_{NaP} = I_{\text{brief late openings}} + I_{\text{bursts}} = (n_1 \cdot p_1 \cdot i) + (n_2 \cdot p_2 \cdot i)$$

To obtain a rough estimate of $I_{NaP}$ amplitude at $-50$ mV, we based our calculations on the following values: $n_1 = 20{,}000$, $n_2 = 22$, $p_1 = 0.0003$, $p_2 = 0.5$, $i = 1.5$ pA. Whereas $i$ and $p$ can be derived from our data, the total number of $Na^+$ channels can only be estimated. Measurements of peak $I_{Na}$ in acutely isolated neocortical cells from rats of similar age have yielded values between 10 and 14 nA (Huguenard et al., 1988). Based on a maximum open probability of 0.6 (Kimitsuki et al., 1990a) and a unitary amplitude of about 1 pA at peak, we estimate that approximately 17,000–23,000 $Na^+$ channels are present on an isolated pyramidal neuron. If all $Na^+$ channels have an identical probability of brief late openings, $n_1$ equals $n$, which we set to 20,000. The probability that a single channel engaged in a brief late opening ($p_1$) was obtained by dividing the average $NP_o$ value (0.0034) by the average number of channels in a patch, which we took as 10. Inactivation failures occurred at an average frequency of 1.1 in 100 depolarizations. Assuming 10 channels per patch, each channel would produce a sustained burst in 0.11% of all depolarizations. Thus, 22 ($=n_2$) of the 20,000 $Na^+$ channels would simultaneously enter the bursting mode during any depolarization. The fractional open time of a bursting channel ($p_2$) at $-50$ mV was set to 0.5, which is close to the mean value determined from our data (0.47). The unitary channel current at $-50$ mV was set to $-1.5$ pA (Fig. 3). Using these parameters, the persistent current mediated by brief late openings is calculated to be 9 pA, whereas sustained bursts produce 16.5 pA. A quite comparable ratio of background to burst current was found in skeletal muscle, where $Na^+$ channels show very similar patterns of late gating (Patlak and Ortiz, 1986).

*Physiological significance of late $Na^+$ channel gating*

Our estimated value of $I_{NaP}$ at $-50$ mV represents only about 0.25% of the peak $I_{Na}$ magnitude. This is comparable to values measured in whole-cell recordings from skeletal muscle and isolated CA1 neurons from hippocampus (Gage et al., 1989; French et al., 1990). Though $I_{NaP}$ is a tiny fraction of the peak $I_{Na}$, it is of great physiological significance for the integrative properties of neocortical neurons because it is present over a voltage range where other voltage- or $Ca^{2+}$-gated currents are small or absent (Stafstrom et al., 1982, 1985). A putative function of $I_{NaP}$ in neocortical neurons is to cause membrane potential to attain a more depolarized value in response to an excitatory synaptic current than it would if the membrane were behaving only passively (Stafstrom et al., 1982). Based on the input resistance (about 1 GΩ) measured in a slice preparation of hippocampal pyramidal neurons of similar age (Edwards et al., 1989), our estimated $I_{NaP}$ at $-50$ mV would tend to depolarize membrane potential by an additional 26 mV. Clearly, late $Na^+$ channel activity can fulfill the role ascribed to $I_{NaP}$. The idea that late $Na^+$ channel openings can provide a meaningful current despite their rare incidence is also supported experimentally by a recent study of ventricular myocytes (Kiyosue and Arita, 1989). As in our preparation, $Na^+$ channels in myocytes display both isolated brief openings and occasional failures of inactivation. These events occurred at an even lower frequency than in our cells, but Kiyosue and Arita (1989) clearly demonstrated that they added up to a small but significant current that contributes to the plateau of the cardiac action potential and affects its duration.

Developmental studies have shown that the expression of RI $Na^+$ channels increases progressively after birth and does not reach a maximum until at least a month later (Beckh et al., 1989). A parallel increase in $I_{NaP}$ is suggested by current-clamp recordings from neocortical pyramidal neurons in brain slices from rats at different developmental stages (McCormick and Prince, 1987). In that study, a TTX-sensitive increase in input resistance with membrane depolarization (the presumed current-clamp correlate of $I_{NaP}$) first appeared late during development and then grew progressively over time. Hence, it is likely that the size of $I_{NaP}$ in adult animals is significantly larger than in the 10–21-d-old rats from which we obtained the bulk of our data. Is the enhanced $I_{NaP}$ of adult animals caused by the same mechanisms we observed in the younger rats? This seems likely based on the few recordings we were able to obtain from pyramidal neurons of adult rat or cat. First, the density of $Na^+$ channels on a given patch was considerably higher in mature neurons. Partially as a consequence of this, but maybe also due to an increased likelihood of channel reopening, the incidence of brief late openings in a patch was about one order of magnitude higher than in patches from young rats. Second, $Na^+$ channels in mature neurons appeared to be more prone to stay in a bursting mode for several consecutive sweeps, whereas such behavior was almost absent in developing neurons. Taken together, these findings suggest that $I_{NaP}$ in adult neurons is larger because there is a greater probability both of brief late openings and inactivation failures in a given membrane area.

*Alternatives to the modal gating hypothesis of $I_{NaP}$*

The mechanism we believe to underlie $I_{NaP}$ in CNS neurons differs from earlier explanations of this phenomenon. In a preliminary study of acutely isolated neocortical cells, Hamill et al. (1986) found repetitive $Na^+$ channel openings only around threshold potentials, suggesting that the persistent $Na^+$ current is a "window" current present only in a narrow range of voltages where $Na^+$ channels were activated but where inactivation was too weak to shut all channels. We could not confirm these findings. Instead, we found brief late openings to occur most frequently between $-40$ and $-20$ mV (Fig. 5*C*). Neither was the incidence of sustained bursts restricted to a small voltage "window" (Fig. 8). During voltage ramps, for example, bursts of openings beginning near $-60$ mV did not cease as the potential gradually dropped to $-20$ mV (Fig. 9). The notion that the persistent openings are distinct from a "window" phenomenon is also supported by whole-cell recordings. French et al. (1990) showed that the $I_{NaP}$ in hippocampal neurons clearly differed from the "window" current predicted by steady-state activation and inactivation of the fast $I_{Na}$. In addition, steady-state $Na^+$ currents in a number of preparations do not fit into the small

"window" allowed by standard Hodgkin and Huxley kinetics (Patlak, 1991).

An alternative proposal to account for $I_{NaP}$ has been recently made by Masukawa et al. (1991). In cell-attached recordings from cultured hippocampal cells, they found a 15–25 pS channel that mediated a noninactivating, Cd- and Co-insensitive inward current. During 120 msec depolarizing steps, this channel type stayed open all the time or made only a few transitions between open and closed states. While Masukawa et al. (1991) observed this channel in about 30% of patches from the somatic region of hippocampal neurons, we did not see a channel displaying a similar gating pattern in any of our patches. The reason for this discrepancy is not immediately obvious, but regional differences (hippocampus vs neocortex) or different recording conditions (cultured cells vs cells *in situ* or acutely dissociated cells) might be possible explanations. The gating shifts of $Na^+$ channels we observed in cortical neurons have, however, been seen in other tissues. In both cardiac and skeletal muscle preparations, $Na^+$ channels failed to inactivate at about the same frequency that we observed, and the inactivation failure consisted of sustained bursts of openings that strikingly resemble the ones described here (Patlak and Ortiz, 1985, 1986; Fozzard et al., 1987; Grant and Starmer, 1987; Kohlhardt et al., 1987; Kiyosue and Arita, 1989). Similar shifts between fast and very slow gating were also observed in purified eel $Na^+$ channels that were reconstituted in artificial liposomes (Correa et al., 1990). Modal gating may thus emerge as a general kinetic feature of $Na^+$ channels independent of their subtype classification.

## References


Aldrich RW, Stevens CF (1987) Voltage-dependent gating of single sodium channels from mammalian neuroblastoma cells. J Neurosci 7:418–431.

Aldrich RW, Corey DP, Stevens CF (1983) A reinterpretation of mammalian sodium channel gating based on single channel recording. Nature 306:436–441.

Alonso A, Llinás RR (1989) Subthreshold $Na^+$-dependent theta-like rhythmicity in stellate cells of entorhinal cortex layer II. Nature 342: 175–177.

Alzheimer C, Schwindt PC, Crill WE (1992) Two gating modes of Na channel openings in neurons from rat neocortex. Biophys J 61:A109.

Attwell D, Cohen I, Eisner D, Ohba M, Ojeda C (1979) The steady state TTX-sensitive ("window") sodium current in cardiac Purkinje fibres. Pfluegers Arch 379:137–142.

Barres BA, Chun LLY, Corey DP (1989) Glial and neuronal forms of the voltage-dependent sodium channel: characteristics and cell-type distribution. Neuron 2:1375–1388.

Beckh S, Noda M, Lübbert H, Numa S (1989) Differential regulation of three sodium channel messenger RNAs in the rat central nervous system during development. EMBO J 8:3611–3616.

Catterall WA (1988) Structure and function of voltage-sensitive ion channels. Science 242:50–61.

Correa AM, Bezanilla F, Agnew WS (1990) Voltage activation of purified eel sodium channels reconstituted into artificial liposomes. Biochemistry 29:6230–6240.

Dascal N, Lotan I (1991) Activation of protein kinase C alters voltage dependence of a $Na^+$ channel. Neuron 6:165–175.

de Leon MS, Chen Y, Tomaselli G, Yue DT (1992) Single-channel properties of a cloned skeletal muscle Na channel ($\mu$I) expressed in a mammalian cell line. Biophys J 61:A108.

Edwards FA, Konnerth A, Sakmann B, Takahashi T (1989) A thin slice preparation for patch clamp recordings from neurones of the mammalian central nervous system. Pfluegers Arch 414:600–612.

Fozzard HA, Hanck DA, Makielski JC, Scanley BE, Sheets MF (1987) Sodium channels in cardiac Purkinje cells. Experientia 43:1162–1168.

French CR, Sah P, Buckett KJ, Gage PW (1990) A voltage-dependent persistent sodium current in mammalian hippocampal neurons. J Gen Physiol 95:1139–1157.

Gage PW, Lamb GD, Wakefield BT (1989) Transient and persistent sodium currents in normal and denervated mammalian skeletal muscle. J Physiol (Lond) 418:427–439.

Grant AO, Starmer CF (1987) Mechanisms of closure of cardiac sodium channels in rabbit ventricular myocytes: single-channel analysis. Circ Res 60:897–913.

Hamill OP, Marty A, Neher E, Sakmann B, Sigworth FJ (1981) Improved patch-clamp techniques for high-resolution current recording from cells and cell-free membrane patches. Pfluegers Arch 391:85–100.

Hamill OP, Huguenard JR, Enayati EF, Prince DA (1986) Single channel currents underlying slow threshold $Na^+$ conductances in rat neocortical neurons. Soc Neurosci Abstr 12:950.

Hille B (1992) Ionic channels of excitable membranes. Sunderland, MA: Sinauer.

Horn R, Vandenberg CA, Lange K (1984) Statistical analysis of single sodium channels—effects of *N*-bromoacetamide. Biophys J 45:323–335.

Huguenard JR, Hamill OP, Prince DA (1988) Developmental changes in $Na^+$ conductances in rat neocortical neurons: appearance of a slowly inactivating component. J Neurophysiol 59:778–795.

Kimitsuki T, Mitsuiye T, Noma A (1990a) Maximum open probability of single $Na^+$ channels during depolarization in guinea-pig cardiac cells. Pfluegers Arch 416:493–500.

Kimitsuki T, Mitsuiye T, Noma A (1990b) Negative shift of cardiac $Na^+$ channel kinetics in cell-attached patch recordings. Am J Physiol 258:H247–H254.

Kirsch GE, Brown AM (1989) Kinetic properties of single sodium channels in rat heart and rat brain. J Gen Physiol 93:85–99.

Kiyosue T, Arita M (1989) Late sodium current and its contribution to action potential configuration in guinea pig ventricular myocytes. Circ Res 64:389–397.

Kohlhardt M, Fröbe U, Herzig JW (1987) Properties of normal and non-inactivating single cardiac $Na^+$ channels. Proc R Soc Lond [Biol] 232:71–93.

Kunze DL, Lacerda AE, Wilson DL, Brown AM (1985) Cardiac Na currents and the inactivating, reopening, and waiting properties of single cardiac Na channels. J Gen Physiol 86:691–719.

Lawrence JH, Yue DT, Rose WC, Marban E (1991) Sodium channel inactivation from resting states in guinea-pig ventricular myocytes. J Physiol (Lond) 443:629–650.

Llinás R, Sugimori M (1980) Electrophysiological properties of *in vitro* Purkinje cell somata in mammalian cerebellar slices. J Physiol (Lond) 305:171–195.

Llinás RR (1988) The intrinsic electrophysiological properties of mammalian neurons: insights into central nervous system function. Science 242:1654–1664.

Masukawa LM, Hansen AJ, Shepherd G (1991) Distribution of single-channel conductances in cultured rat hippocampal neurons. Cell Mol Neurobiol 11:231–243.

McCormick DA, Prince DA (1987) Post-natal development of electrophysiological properties of rat cerebral cortical pyramidal neurones. J Physiol (Lond) 393:743–762.

Moorman JR, Kirsch GE, VanDongen AMJ, Joho RH, Brown AM (1990) Fast and slow gating of sodium channels encoded by a single mRNA. Neuron 4:243–252.

Neumcke B (1990) Diversity of sodium channels in adult and cultured cells, in oocytes and in lipid bilayers. Rev Physiol Biochem Pharmacol 115:1–49.

Nilius B (1988) Modal gating behavior of cardiac sodium channels in cell-free membrane patches. Biophys J 53:857–862.

Numann R, Catterall WA, Scheuer T (1991) Functional modulation of brain sodium channels by protein kinase C phosphorylation. Science 254:115–118.

Ono K, Fozzard HA (1991) Late current through $Na^+$ channels modified by forskolin. Biophys J 59:72a.

Patlak J (1991) Molecular kinetics of voltage-dependent $Na^+$ channels. Physiol Rev 71:1047–1080.

Patlak JB, Ortiz M (1985) Slow currents through single sodium channels of the adult rat heart. J Gen Physiol 86:89–104.

Patlak JB, Ortiz M (1986) Two modes of gating during late $Na^+$ channel currents in frog sartorius muscle. J Gen Physiol 87:305–326.

Patlak JB, Ortiz M (1989) Kinetic diversity of $Na^+$ channel bursts in frog skeletal muscle. J Gen Physiol 94:279–301.

Plummer MR, Hess P (1991) Reversible uncoupling of inactivation in N-type calcium channels. Nature 351:657–659.

Quandt FN (1987) Burst kinetics of sodium channels which lack fast

inactivation in mouse neuroblastoma cells. J Physiol (Lond) 392:563–585.

Sayer RJ, Schwindt PC, Crill WE (1990) High- and low-threshold calcium currents in neurons acutely isolated from rat sensorimotor cortex. Neurosci Lett 120:175–178.

Scanley BE, Hanck DA, Chay T, Fozzard HA (1990) Kinetic analysis of single sodium channels from canine cardiac Purkinje cells. J Gen Physiol 95:411–437.

Sigworth FJ, Neher E (1980) Single $Na^+$ channel currents observed in cultured rat muscle cells. Nature 287:447–449.

Stafstrom CE, Schwindt PC, Crill WE (1982) Negative slope conductance due to a persistent subthreshold sodium current in cat neocortical neurons *in vitro*. Brain Res 236:221–226.

Stafstrom CE, Schwindt PC, Flatman JA, Crill WE (1984) Properties of subthreshold response and action potential recorded in layer V neurons from cat sensorimotor cortex *in vitro*. J Neurophysiol 52: 244–263.

Stafstrom CE, Schwindt PC, Chubb MC, Crill WE (1985) Properties of persistent sodium conductance and calcium conductance of layer V neurons from cat sensorimotor cortex *in vitro*. J Neurophysiol 53: 153–170.

Ukomadu C, Zhou J, Sigworth FJ, Agnew WS (1992) $\mu$I $Na^+$ channels expressed transiently in human embryonic kidney cells: biochemical and biophysical properties. Neuron 8:663–676.

Westenbroek RE, Merrick DK, Catterall WA (1989) Differential subcellular localization of the $R_I$ and $R_{II}$ $Na^+$ channel subtypes in central neurons. Neuron 3:695–704.

Zhou J, Potts JF, Trimmer JS, Agnew WS, Sigworth FJ (1991) Multiple gating modes and the effect of modulating factors on the $\mu$I sodium channel. Neuron 7:775–785.